Environment International 181 (2023) 108272

Contents lists available at ScienceDirect

Environment International

journal homepage: www.elsevier.com/locate/envint

Full length article

Early life exposure to F-53B induces neurobehavioral changes in developing children and disturbs dopamine-dependent synaptic signaling in weaning mice

Li-Xia Liang [a,1], Jingjing Liang [b,1], Qing-Qing Li [a,1], Mohammed Zeeshan [a,c,1], Zheqing Zhang [d], Nanxiang Jin [e], Li-Zi Lin [a], Lu-Yin Wu [a], Ming-Kun Sun [a], Wei-Hong Tan [f], Yang Zhou [g], Chu Chu [a], Li-Wen Hu [a], Ru-Qing Liu [a], Xiao-Wen Zeng [a,*], Yunjiang Yu [g,*], Guang-Hui Dong [a,*]

[a] *Guangdong Provincial Engineering Technology Research Center of Environmental Pollution and Health Risk Assessment, Department of Occupational and Environmental Health, School of Public Health, Sun Yat-sen University, Guangzhou 510080, China*
[b] *Department of Child Health Care, Guangzhou Women and Children's Medical Center, Guangzhou Medical University, Guangzhou, China*
[c] *Developmental Biology and Genetics, Indian Institute of Science, Bangalore, India*
[d] *Department of Nutrition and Food Hygiene, Guangdong Provincial Key Laboratory of Tropical Disease Research, School of Public Health, Southern Medical University, Guangzhou, China*
[e] *A.I.Virtanen Institute for Molecular Science, University of Eastern Finland, Neulaniementie 2, 70210 Kuopio, Finland*
[f] *Department of Reproductive Medicine and Genetics Center, The People's Hospital of Guangxi Zhuang Autonomous Region, Nanning, China*
[g] *State Environmental Protection Key Laboratory of Environmental Pollution Health Risk Assessment, South China Institute of Environmental Sciences, Ministry of Ecology and Environment, Guangzhou 510655, China*

ARTICLE INFO

Handling Editor: Adrian Covaci

Keywords:
F-53B
Neurotoxicity
Synaptic plasticity
Dopamine

ABSTRACT

Background: Previous studies have shown that F-53B exposure may be neurotoxic to animals, but there is a lack of epidemiological evidence, and its mechanism needs further investigation.
Methods: Serum F-53B concentrations and Wisconsin Card Sorting Test (WCST) were evaluated in 314 growing children from Guangzhou, China, and the association between them were analyzed. To study the developmental neurotoxicity of F-53B, experiments on sucking mice exposed via placental transfer and breast milk was performed. Maternal mice were orally exposed to 4, 40, and 400 μg/L of F-53B from postnatal day 0 (GD0) to postnatal day 21 (PND 21). Several genes and proteins related to neurodevelopment, dopamine anabolism, and synaptic plasticity were examined by qPCR and western blot, respectively, while dopamine contents were detected by ELISA kit in weaning mice.
Results: The result showed that F-53B was positively associated with poor WCST performance. For example, with an interquartile range increase in F-53B, the change with 95 % confidence interval (CI) of correct response (CR), and non-perseverative errors (NPE) was −2.47 (95 % CI: −3.89, −1.05, $P = 0.001$), 2.78 (95 % CI: 0.79, 4.76, $P = 0.007$), respectively. Compared with the control group, the highest exposure group of weaning mice had a longer escape latency (35.24 s vs. 51.18 s, $P = 0.034$) and a lesser distance movement (34.81 % vs. 21.02 %, $P < 0.001$) in the target quadrant, as observed from morris water maze (MWM) test. The protein expression of brain-derived neurotrophic factor (BDNF) and growth associated protein-43 (GAP-43) levels were decreased, as compared to control (0.367-fold, $P < 0.001$; 0.366-fold, $P < 0.001$; respectively). We also observed the upregulation of dopamine transporter (DAT) (2.940-fold, $P < 0.001$) consistent with the trend of dopamine content (1.313-fold, $P < 0.001$) in the hippocampus.

* Corresponding authors at: Guangdong Provincial Engineering Technology Research Center of Environmental Pollution and Health Risk Assessment, Guangzhou Key Laboratory of Environmental Pollution and Health Risk Assessment, Department of Preventive Medicine, School of Public Health, Sun Yat-sen University, 74 Zhongshan 2nd Road, Yuexiu District, Guangzhou 510080, China (X.-W. Zeng). State Environmental Protection Key Laboratory of Environmental Pollution Health Risk Assessment, South China Institute of Environmental Sciences, Ministry of Environmental Protection, Guangzhou 510655, China (Y. Yu). Guangdong Provincial Engineering Technology Research Center of Environmental Pollution and Health Risk Assessment, Department of Occupational and Environmental Health, School of Public Health, Sun Yat-sen University, 74 Zhongshan 2nd Road, Yuexiu District, Guangzhou 510080, China (G.-H. Dong).
E-mail addresses: zxw63@mail.sysu.edu.cn (X.-W. Zeng), yuyunjiang@scies.org (Y. Yu), donggh5@mail.sysu.edu.cn (G.-H. Dong).
[1] These authors contributed equally to this work and should be listed as first authors.

https://doi.org/10.1016/j.envint.2023.108272
Received 16 May 2023; Received in revised form 2 September 2023; Accepted 16 October 2023
Available online 17 October 2023

Conclusion: Early life exposure to F-53B is associated with adverse neurobehavioral changes in developing children and weaning mice which may be modulated by dopamine-dependent synaptic plasticity.

1. Introduction

Chlorinated poly-fluoroalkyl ether sulfonic acid (Cl-PFESAs) composed of 6:2 and 8:2Cl-PFESAs and traded under the name of F-53B, is widely used as an alternative to perfluorooctane sulfonate (PFOS). Cl-PFESAs was first synthesized in China in 1970s (Wang et al., 2013). Since then, it is widely used in various industries and detected in different environmental and human samples, such as ambient air (Liu et al., 2017), surface water (Zhou et al., 2019b), sewage sludge (Ruan et al., 2015), sediment (MacInnis et al., 2019), human blood (whole blood, plasma, and serum) (Liu et al., 2021)(Liu et al., 2022), breast milk (Awad et al., 2020), placenta (Lu et al., 2021), urine, nail, and hair (Wang et al., 2018b). In addition, F-53B is recognized as the most persistent per- and polyfluoroalkyl substances (PFASs), with a long total elimination time of 15.3 year (Shi et al., 2016). Due to its ubiquitous presence and strong persistence, its toxic effects have attracted broad attention. Previous studies have shown that F-53B exposure may exert neurotoxic effects. Zhang et al., 2016 reported that acute short-term exposure to 6:2 Cl-PFESA inhibited long-term potentiation (LTP) in the hippocampal CA1 region of adult rats, leading to synaptic plasticity damage (Zhang et al., 2016). Further, 6:2 Cl-PFESA inhibited the expression of neural marker genes in embryonic stem cells (ESCs) and affected the normal differentiation of nerve stems (Yin et al., 2018). However, there is a lack of epidemiological evidence on the neurotoxicity of F-53B, and its mechanism needs further investigation.

The nervous system is sensitive to exogenous chemicals, especially during early childhood. The development of the nervous system is easily affected by environmental toxic chemicals (Zhou et al., 2019a)(Yuan et al., 2022). Although the pathway of human exposure to F-53B is not well clear, *trans*-placental transmission and breastfeeding are two vital routes causing early-life exposure (Cai et al., 2020; He et al., 2022; Jin et al., 2020a). Once in the human body, F-53B shows high protein-binding affinity with human serum albumin (Sheng et al., 2020) and can be efficiently transported across placenta and brain barrier (Wang et al., 2018a), which may cause potential neural damage. Hence, pregnancy and lactation are two key periods for the study of nerve damage in early life caused by F-53B.

6:2 Cl-PFESA, the main component of F-53B, has been reported to impair synaptic plasticity in adult rats (Zhang et al., 2016). Synaptic plasticity, the ability of individual synaptic connections to use or discard transmission along synaptic pathways, is associated with spatial learning and memory (Wang et al., 2015). Previous studies have shown that dopamine (DA) regulates synaptic plasticity in different brain regions, such as the striatum, hippocampus, and cortex (Calabresi et al., 2007; Huang et al., 2004; Li et al., 2003). DA neurotransmitter system, a potential target of environmental chemicals, has been shown to produce motoric and cognitive impairments in animals (Hallgren and Viberg, 2016; Umegaki et al., 2001). Moreover, many neuropsychiatric disorders such as attention deficit and hyperactivity disorder (ADHD) and autism spectrum disorder in children are treated with medicines that act via dopamine anabolic pathways (Babcock et al., 2012; Rubia et al., 2011). However, it remains unclear whether the alteration in plasticity caused by F-53B are tied to the dopamine system and which specific brain region is predominantly affected.

To address these knowledge gaps, the current study was conducted with the following objective: (1) Assess the impact of F-53B exposure on neurobehavioral deficits during early life in children and weaning mice; (2) Establish a correlation between neurobehavioral deficits and functional changes in brains of mice with a focus on the striatum, hippocampus, and cortex; (3) Probe the possible mechanisms associated with dopamine-dependent synaptic plasticity.

2. Materials and methods

2.1. Subjects and sample collection

In this cross-sectional study, we enrolled children from several elementary school in urban Guangzhou, China. The following selection criteria were applied in the present study; (1) Age $\geq$ 6 years old; (2) The score of Intelligence Quotient (IQ) > 70; (3) Free from color amblyopia or color-blindness; (4) Without development and neuropsychiatric disorders based on parental questionnaires (e.g., development delay, attention deficit syndrome, depression); (5) Non-twins; (6) Willing to provide a blood sample. A total of 337 children were enrolled for the study. Both the children and their parents participated in an interview-administered questionnaire. The questionnaire collected information such as child's age (year), sex (boy/girl), height (cm), weight (kg), maternal age (age of pregnant woman at the birth; in years), details about the infant feeding pattern for the first six months (breastfeeding / formula-fed), gestational age (preterm / term), and the mode of delivery (eutocia / caesarean). Physical activity was assessed using a 3-day (one weekend day and two weekdays) questionnaire and documented the type and duration of each physical activity. Metabolic equivalent task values ($\sum$metabolic equivalent fractions; kcal/kg/hour) were calculated for each physical activity by multiplying the metabolic equivalent fraction by the duration (in hours) per day (Ainsworth et al., 2011). Participants were also shown food pictures depicting portion sizes, and energy intake was calculated by the 2009 China Food Composition table (Chen et al., 2022). Twenty-three children were excluded due to missing information, of these, 17 did not complete the working memory/executive function test known as the Wisconsin Card Sorting Test (WCST), and 6 missed basic information. Finally, 314 children were included in our analyses. This study was approved by the Ethnic Committee of the School of Public Health, Sun Yat-sen University (NO. 201549). The flow chart of this study was provided in Figure S1.

2.2. Wisconsin card sorting test

The WCST is a neuropsychological test widely used to measure working memory/executive function (Egan et al., 2001). Poor performance on the WCST can reflect difficulties in concept formation, sustained attention, learning, working memory, and task switching (Grön, 1998; Smith et al., 1998; Sullivan et al., 1993). The participants were asked to sort 128 cards according to their number, shape, and color. All the operations were done on the computer. Through the feedback on the computer screen, "$\surd$" or "$\times$", participants need to judge the card sorting rules by themselves. After ten successive correct reactions, the rules changed automatically. The test ends when six categories are completed successfully or all cards are used up (Dai et al., 2019). Twelve WCST indexes were used for analysis (Table S1).

2.3. F-53B measurements

The concentration of F-53B in the serum of children, as well as in the serum and breast milk of mice, were measured according to Benskin et al (Benskin et al., 2012), with slight modifications. Briefly, we measured the concentration of F-53B using 200 μL serum and quantified it by ultra-performance liquid chromatography attached to an Agilent 6495B Triple Quadrupole tandem mass spectrometer (Palo Alto and Santa Clara, CA USA). We defined the limit of detection (LOD) as the measurable

concentration of the serum that gets to a peak with a signal-to-noise ratio of 3 (S/N = 3). For concentration below the LOD, data were represented as $LOD/\sqrt{2}$. Detection of F-53B in mouse placenta was carried by a similar approach: approximately 10 mg of tissue was excised, its mass was recorded, and then the tissue was ground. Following this, 1 mL of acetonitrile was added for further grinding. Subsequently, vortex-oscillating centrifugation was conducted, and the resulting supernatant was collected for subsequent experimentation. The remaining procedures were consistent with the aforementioned methodology. Detailed information is presented in the Supplementary Material.

2.4. Animal experiments

Eighty C57BL/6 mice (7–8 weeks old, 18–22 g, female: male = 1:1) were purchased from Guangdong Medical Laboratory Animal Center. After adaptive feeding (24–25 °C room temperature and 12 h/daylighting) for 1 week, the mice were mated in cages. Gestation day 0 (GD 0) was determined by vaginal smear microscopy. Pregnant mice were randomly assigned into four groups with 10 mice in each group. The calculation of the F-53B dose was based on a previous article (Lai and Lee, 2017). In brief, Oral dose = human tolerable daily intake (HED) * uncertainty factor for human (UFH)* uncertainty factor for interspecies (UFI)* uncertainty factor for toxicokinetics (UFT). However, since physiologically based pharmacokinetic (PBPK) model of F-53B is not available, some parameters used for dose estimation were adopted from the PBPK model of PFOS (US EPA, 2016). Where HED = average serum concentration (in ug/mL) * Clearance rate (CL; in mL/kg/day)); CL = a volume of distribution (V_d) × (0.693 ÷ half-life ($t_{1/2}$)); V_d: 0.23 L/kg and 268 mL/kg for human and mice, respectively; $T_{1/2}$: 15.3 years × 365 days/year and 36.9 days for human and mice, respectively. UFH: a correction factor of 10×. UFI: human vs. mice; a correction factor of 3×. UFT = CL_{mice}/ CL_{human} (a correction factor of 176.6 ×). Based on the general adult (4.78 ng/mL) and occupational people (51.5 ng/mL) levels (Shi et al., 2016), an equivalent dose of 0.72 and 7.78 μg/kg was defined. Considering pre-pregnancy weight (20 g) and the volume daily water intake of mice (4 mL), the exposure dose was converted into drinking water exposure concentration of 4 μg/L and 40 μg/L, and a dose of 0 μg/L (0.5 %Tween 20) and 400 μg/L was added. Animals were administered F-53B dissolved in water every day. Breast milk was collected from three pregnant mice in each group (except 400 μg/L dose group), and placenta along with fetal liver were dissected on GD14. After birth (postnatal day 0, PND0), remaining postpartum mice continued with respective doses of F-53B and were exposed until PND21 (weaning). Weaning mice were exposed to F-53B through the placenta and breast milk. Ten weaning mice from each dose were included in subsequent analyses. For details, see Figure S2. The mice were recorded daily, such as weight and litter number. At the end of the experiment, the tissue of both maternal and weaning mice was dissected, such as heart, liver, stomach, thymus, lung, kidney, spleen and brain.

2.5. Open field test

An open field exposure was conducted at PND21 to evaluate the motor ability and exploratory behavior of the weaning mice. The experimental apparatus consists of an open field chamber, automatic data acquisition, and a data processing system (PhenoScan, Clever Sys., Inc, USA). The chamber was composed of four sub-reaction chambers of the same size (length * width * height = 40 cm *40 cm *40 cm). The digital camera is located 2 m above the apparatus to capture the movement of animals in all the chambers. The weaning mice were acclimated in the lab for half an hour before the start of the experiment, and the chambers were wiped with alcohol to remove odor cues left by other weaning mice. At the beginning of each test, every animal was introduced to the center of the apparatus and was allowed to explore the chambers. For 10 min, the movement distance travelled and speed were analyzed.

2.6. Morris water maze

Morris water maze (MWM) consists of three parts: a circular pool, a safety island, and a recording system. The pool was virtually divided into 4 quadrants. Above the maze is a video camera, connected to a computer. The recording system in the computer is the behavioral detection module provided by Clever Sys. (PhenoScan, Clever Sys., Inc, USA), which can automatically input and analyze the swimming trajectory. On PND21, it was adaptive swimming. The weaning mice were introduced into a pool without safe island for 1 min to adapt to the water environment. The positioning navigation experiment was conducted with 2 trials per day over 4 days. The safety island was 1 cm above the water and fixed in the same position. The four quadrants of the pool were successively used as entry points, and the time it took to find and climb the safety island (escape latency) was recorded. If the animals fail to find the safety island within 60 s, assistance was provided to help animals reach the safety island and recorded the time as 60 s. The average of the four times was taken as the academic performance. On PND26, the safety island was hidden 1 cm below the surface of water. The midpoint of the diagonal quadrant of the safety island was selected as the water entry point, and the time from water entry to the position of the safety island was recorded. On PND27, the safety island was withdrawn, and the mice was allowed to swim freely for 60 s. The escape latency, swimming speed (cm/s) and distance (cm) were recorded by the camera and used to evaluate the learning and spatial memory.

2.7. Gene expression analysis

The mRNA was extracted using the Trizol Reagent kit (Invitrogen, US) and transcribed into cDNA with ReverTra Ace® qPCR RT kit (TOYOBO, China). Nanodrop 2000 (Thermo Fisher Scientific, US) was used to measure the concentration and control quality for RNA. Quantitative real-time PCR was performed using SYBR® Green Realtime PCR Master Mix (TOYOBO, China) and QuantStuadio 7 Flex (Thermo Fisher Scientific, US). β-actin was selected to normalize the RNA levels. The primer sequences (Tsingke Biotechnology, China) are listed in Table S3.

2.8. Protein expression analysis

Total protein was extracted and quantified using a commercial Enhanced BCA Protein Assay Kit (Beyotime, China). Protein was electrophoresed on a 10 % SDS polyacrylamide gel and then transferred onto polyvinylidene difluoride membranes (PVDF) membranes (Millipore, US). Blocking was performed for 2 h with Antibody Blocking Solution (Beyotime, China) at room temperature, and the membranes were incubated with primary antibodies overnight at 4 °C. Finally, HRP-conjugated goat anti-rabbit or anti-mouse IgG (Solarbio Lifescience, China) was incubated for 2 h at room temperature, and membranes were visualized by ODYSSEY 9120 (LI-COR). β-actin was selected to normalize the protein levels. The antibodies of interest were GAPDH (GeneTex, 1:5000), BDNF (Proteintech, 1:1000), TH (GeneTex, 1:1000), DAT (GeneTex, 1:1000), and GAP-43 (Proteintech, 1:1000).

2.9. Dopamine measurement

Dopamine in the hippocampus, cortex, and striatum was measured by enzyme-linked immunosorbent assay (Mouse Dopamine ELISA Kit; Meike, Jiangsu Sumeike Biological Technology Co., Ltd, China) following the collection of tissue specimens. All steps were carried out according to the manufacturer's instructions. The content of dopamine was detected within 15 min after adding the stop solution, and the absorbance (OD) of each well was measured at 450 nm using an absorption photomicroplate reader 800TS (BioTek Synergy H1; Agilent Technologies, USA).

2.10. Statistic analysis

For human cohort study, data analyses were performed using the R software version 4.1.2 (Foundation for Statistical Computing, US). The normality of continuous data was examined by the Shapiro-Wilk test. We used *t*-tests and Wilcoxon rank-sum to compare the value in normally distributed variables and skewed variables, respectively, across sex. While χ2-test was used for categorical variables. We applied generalized linear models (GLMs) to explore the association between F-53B and WCST index with adjustment for the child's age, sex, body mass index (BMI, in kg/m^2), energy intake, metabolic equivalent task, maternal age, feeding pattern, gestational age, and birth delivery mode. The concentration of F-53B was categorized as a quartile of increasing chemistry and evaluated the estimated WCST index with 95 % confidence intervals (CI) with one quartile of F-53B increased. For animal studies, data were analyzed by SPSS version 20.0 (IBM) and histograms were created using GraphPad Prism 6 (GraphPad Software). The differences between the treatment and the control groups were analyzed by one-way ANOVA followed by the LSD post hoc test. Data were expressed as mean ± SD, and $P < 0.05$ was selected as the threshold for statistical significance.

3. Results

3.1. Characterization of children

A total of 314 growing children (173 boys and 141 girls) were included in our analyses. The mean age of the children was 8.08 years and over 80 % of them were breastfed for the first six months of life. As compared to girls, boys had higher BMI (15.32 vs. 14.50 kg/m^2, $P < 0.001$), higher energy intake (43.11 vs. 37.02 kcal/d, $P = 0.017$), and higher NET (40.07 vs. 38.22 kcal·d^{-1}·kg^{-1}, $P = 0.002$). The median concentrations with interquartile range (IQR) of F-53B, 6:2Cl-PFESA and 8:2Cl-PFESA were 1.12 (0.74, 1.80), 1.10 (0.72, 1.76) ng/mL and 0.02 (0.01, 0.04) ng/mL, respectively. However, the median concentration of F-53B was not statistically significant across sex (Table 1).

3.2. Association between F-53B and WCST index in children

F-53B was negatively associated with CR, PCR, and PCLR, while positively with RE, NPE, PNPE, and PR. With an interquartile range (IQR) increase in F-53B, CR, PCR, PCLR, RE, NPE, PNPE, and PR were changed by −2.47 (95 % CI: −3.89, −1.05, $P = 0.001$), −2.09 (95 % CI:-3.47, −0.71, $P = 0.003$), −2.35 (95 % CI: −4.04, −0.66, $P = 0.007$), 2.77 (95 % CI: 0.84, 4.71, $P = 0.005$), 2.78 (95 % CI: 0.79, 4.76, $P = 0.007$), 0.02 (95 % CI: 0.01, 0.04, $P = 0.005$), and 1.03 (95 % CI: 0.13, 1.93, $P = 0.025$), respectively (Table 2).

3.3. Effect of F-53B exposure on motor and learning ability of weaning mice

In the open field experiment, compared with the control group, the exposed animals (4 μg/L, 40 μg/L, and 400 μg/L) travelled a longer distance (14.54 m vs. 21.10 m, 22.21 m, and 19.62 m), with a greater speed (24.80 mm/s vs. 35.46 mm/s, 37.97 mm/s, and 33.42 mm/s). Further, the exposed animals spent a greater proportion of time in the inner quadrant (23.75 % vs. 33.57 %, 36.45 %, and 31.63 %) and a lower proportion of time in the outer quadrant (60.45 % vs. 48.22 %, 54.81 %, and 50.71 %) (Fig. 1A-1D).

In the MWM test, when compared with the control group, the exposed animals (400 μg/L group) exhibited a significantly longer escape latency (35.24 s vs. 51.18 s, $P = 0.034$). Additionally, the mice in the 400 μg/L exposed group traveled a longer distance (34.81 % vs. 21.02 %, $P < 0.001$) and spent more time in the target quadrant (34.15 % vs. 20.46 %, $P < 0.001$) (Fig. 1G-1I).

Table 1
Characteristics of the study participants (n = 314).

Character	Total (n = 314)	Boys (n = 173, 55.10 %)	Girls (n = 141, 44.90 %)	*P* value
Age (years), (mean ± SD)	8.08 ± 0.96	8.02 ± 0.98	8.15 ± 0.93	0.221
BMI (kg/m^2), median (Q1, Q3)	15.04 (13.99, 16.41)	15.32 (14.20, 16.958)	14.50 (13.66, 15.89)	**<0.001**
Maternal Age (years)	28.16 ± 3.67	27.98 ± 3.65	28.38 ± 3.70	0.339
Energy intake (kcal/d), median (Q1, Q3)	40.66 (31.50, 54.45)	43.11 (33.43, 54.82)	37.02 (29.99, 52.88)	**0.017**
MET (kcal·d^{-1}·kg^{-1}), median (Q1, Q3)	39.05 (37.11, 42.16)	40.07 (37.45, 42.85)	38.22 (36.53, 41.33)	**0.002**
Eutocia (%)	152 (48.41 %)	81 (46.82 %)	71 (50.35 %)	0.533
Breast feeding (%)	265 (84.39 %)	152 (87.86 %)	113 (80.14 %)	0.061
Preterm (%)	3 (0.96 %)	2 (1.16 %)	1 (0.71 %)	0.686
WCST test, median (Q1, Q3)				
CC	5.00 (3.00, 6.00)	5.00 (3.00, 6.00)	5.00 (4.00, 6.00)	**0.018**
CR	74.00 (64.00, 83.00)	75.00 (63.00, 84.00)	72.00 (66.00, 82.00)	0.666
PCR	65.54 (53.13, 75.00)	64.84 (50.78, 73.68)	65.63 (54.69, 75.23)	0.275
PCLR	60.16 (45.51, 71.88)	59.38 (43.75, 71.03)	61.72 (48.44, 71.88)	0.210
L-L	0.06 (0.02, 0.18)	0.06 (0.02, 0.16)	0.07 (0.02, 0.20)	0.655
RA	128.00 (111.25, 128.00)	128.00 (116.00, 128.00)	128.00 (107.00, 128.00)	**0.038**
RE	44.00 (28.00, 60.00)	45.00 (30.00, 63.00)	43.00 (27.00, 59.00)	0.162
PE	6.00 (5.00, 8.00)	6.00 (5.00, 8.00)	6.00 (5.00, 7.00)	0.821
PPE	5.47 (3.91, 6.58)	5.47 (3.91, 6.45)	5.47 (4.08, 6.67)	0.509
NPE	38.00 (21.00, 54.00)	39.00 (23.00, 56.00)	35.00 (21.00, 52.00)	0.152
PNPE	29.69 (19.14, 42.19)	30.47 (22.31, 43.75)	28.13 (18.35, 40.63)	0.222
PR	14.00 (10.00, 22.00)	14.00 (11.00, 22.00)	14.00 (9.00, 21.00)	0.167
Pollutants (ng/Ml), median (Q1, Q3)				
[a] F-53B	1.12 (0.74, 1.80)	1.09 (0.73, 1.76)	1.13 (0.76, 1.82)	0.405
6:2Cl-PFESA	1.10 (0.72, 1.76)	1.09 (0.71, 1.74)	1.12 (0.74, 1.80)	0.407
8:2Cl-PFESA	0.02 (0.01, 0.04)	0.02 (0.00, 0.03)	0.02 (0.01, 0.04)	0.055

Detailed information on WCST test and pollutants is provided in Table S1 and Table S2, respectively. [a] F-53B values represent summed concentrations of 6:2Cl-PFESA and 8:2Cl-PFESA.

*Abbreviations: BMI, body mass index; MET, Metabolic equivalent task; WCST, Wisconsin card sorting test; CI, Confidence interval; CC, Categories completed; CR, Correct response; PCR, Percent correct response; PCLR, Percent conceptual level response; L-L, Learning to learn; FMS, Failure to maintain set; RA, Response administered; RE, Response errors; PE, Perseverative errors; PPE, Percent perseverative errors; NPE, Non-perseverative errors; PNPE, Percent non-perseverative errors; PR, Perseverative response.

Bold text indicates that the associations were statistically significant at $P < 0.05$.

[a] Models were adjusted for age, sex, BMI, maternal age, energy intake, MET,

feeding pattern, gestational age, and birth delivery mode.
Bold text indicates that the associations were statistically significant at $P < 0.05$.

Table 2
Changes (mean and 95 % CI) in WCST test associated with an interquartile range increase in F-53B (ng/mL).

Index	[a] F-53B	*P* value	[a] 6:2Cl-PFESA	*P* value	[a] 8:2Cl-PFESA	*P* value
CC	−0.14 (−0.28, 0.00)	0.053	−0.14 (−0.28, 0.01)	0.069	**−0.05 (−0.09, −0.01)**	**0.022**
CR	**−2.47 (−3.89, −1.05)**	**0.001**	**−2.49 (−3.94, −1.03)**	**0.001**	**−0.52 (−0.95, −0.09)**	**0.017**
PCR	**−2.09 (−3.47, −0.71)**	**0.003**	**−2.07 (−3.48, −0.66)**	**0.004**	**−0.57 (−0.98, −0.16)**	**0.001**
PCLR	**−2.35 (−4.04, −0.66)**	**0.007**	**−2.32 (−4.05, −0.59)**	**0.009**	**−0.61 (−1.17, −0.04)**	**0.010**
L-L	0.02 (−0.02, 0.06)	0.386	0.02 (−0.02, 0.06)	0.420	0.01 (−0.01, 0.02)	0.268
RA	0.31 (−1.04, 1.66)	0.655	0.24 (−1.14, 1.62)	0.734	0.28 (−0.12, 0.68)	0.172
RE	**2.77 (0.84, 4.71)**	**0.005**	**2.73 (0.74, 4.71)**	**0.001**	**0.80 (0.22, 1.38)**	**0.007**
PE	−0.01 (−0.22, 0.20)	0.937	0.00 (−0.22, 0.22)	0.986	−0.03 (−0.10, 0.03)	0.294
PPE	0.00 (0.00, 0.00)	0.830	0.00 (0.00, 0.00)	0.927	0.00 (0.00, 0.00)	0.160
NPE	**2.78 (0.79, 4.76)**	**0.007**	**2.72 (0.68, 4.76)**	**0.001**	**0.83 (0.24, 1.43)**	**0.006**
PNPE	**0.02 (0.01, 0.04)**	**0.005**	**0.02 (0.01, 0.04)**	**0.001**	**0.01 (0.00, 0.01)**	**0.007**
PR	**1.03 (0.13, 1.93)**	**0.025**	**1.04 (0.13, 1.97)**	**0.026**	0.18 (−0.09, 0.45)	0.198

Detailed information on WCST test and F-53B is provided in Table S1 and Table S2, respectively. F-53B values represent summed concentrations of 6:2Cl-PFESA and 8:2Cl-PFESA.
Abbreviations: BMI, body mass index; MET, Metabolic equivalent task; WCST, Wisconsin card sorting test; CI, Confidence interval; CC, Categories completed; CR, Correct response; PCR, Percent correct response; PCLR, Percent conceptual level response; L-L, Learning to learn; FMS, Failure to maintain set; RA, Response administered; RE, Response errors; PE, Perseverative errors; PPE, Percent perseverative errors; NPE, Non-perseverative errors; PNPE, Percent non-perseverative errors; PR, Perseverative response.
Bold text indicates that the associations were statistically significant at $P < 0.05$.
[a] Models were adjusted for age, sex, BMI, maternal age, energy intake, MET, feeding pattern, gestational age, and birth delivery mode.

3.4. Effects of F-53B exposure on brain damage for weaning mice

There was no statistical difference in ponderal growth and pregnancy period among the four groups. However, the birth weight of weaning mice in the highest dose group (400 μg/L) was decreased compared with the control group (1.39 g vs. 1.27 g, $P < 0.001$) (Table S4). The brain organ coefficients of maternal and weaning mice were increased as compared with the control (Table S5, S6). Further, exposure to 400 μg/L/F-53B significantly down regulated transcriptions of BDNF (0.744-fold, $P < 0.001$), NT-3 (0.756-fold, $P = 0.023$), and NT-4/5 (0.478-fold, $P = 0.030$) in the hippocampus, and also decreased the mRNA levels of BDNF (0.538-fold, $P = 0.016$), NT-3 (0.565-fold, $P = 0.015$), NT-4/5 (0.470-fold, $P = 0.045$) in the cortex. However, in the striatum, a decrease in NT-4/5 expression was seen only at 4 μg/L (0.399-fold, $P = 0.035$) and 40 μg/L (0.202-fold, $P = 0.010$), as compared with the control. Western blot analyses revealed, exposure to 4, 40, and 400 μg/L/F-53B significantly decreased the BDNF expression by 0.657-fold ($P < 0.001$), 0.446-fold ($P < 0.001$), and 0.367-fold ($P < 0.001$) in the hippocampus, respectively. Whereas, in cortex, a decrease of 0.638-fold ($P = 0.009$) and 0.629-fold ($P = 0.008$) was observed only at 40 and 400 μg/L/F-53B, respectively. (See Fig. 2).

3.5. Effects of F-53B exposure on synaptic plasticity for weaning mice

Exposure to F-53B impaired synaptic plasticity in the different brain regions and at different exposures in the weaning mice. In the hippocampus, as compared with control, exposure to 4, 40 and 400 doses μg/L downregulated the expression of GAP-43 (0.712-fold, $P = 0.012$; 0.753-fold, $P = 0.024$; 0.723-fold, $P = 0.015$; respectively), SYP (0.723-fold, $P = 0.011$; 0.598-fold, $P = 0.001$; 0.517-fold, $P < 0.001$; respectively), and PSD-95 (0.797-fold, $P = 0.005$; 0.713-fold, $P = 0.001$; 0.758-fold, $P = 0.002$; respectively). GAP-43 and SYP genes in the cortex also showed a downward trend at the highest exposure group compared with the control group (0.660-fold, $P = 0.017$; 0.660-fold, $P = 0.022$). Whereas, in striatum, only GAP-43 gene was significantly downregulated (0.736-fold, $P = 0.032$), at 40 μg/L/F-53B (Fig. 3A-C).

For protein expression studies, we also observed a significant downregulation of GAP-43 expression in the hippocampus. As compared with control, 40 and 400 μg/L exposure led to decrease of 0.409-fold and 0.366-fold of GAP-43 expression, respectively (Fig. 3D, E).

3.6. Effects of F-53B exposure on DA signaling pathway for weaning mice

TH genes only increased in the striatum and in the highest dose group as compared with control group (1.670-fold, $P = 0.028$) (Fig. 4A). DDC and VMAT2 transcript levels didn't change, in any brain regions or at any exposure (Fig. 4B, 4C). The expression of enzymatic inactivated genes (MAO-A, and COMT) and dopamine receptors decreased (0.651-fold, $P = 0.016$; 0.780-fold, $P = 0.040$; respectively) at 400 μg/L/F-53B in hippocampus, while the transporter (DAT) increased at 400 μg/L/F-53B in cortex and stratum (6.115-fold, $P = 0.005$; 5.980-fold, $P = 0.015$; respectively) (Fig. 4D-4L).

Exposure to 40 μg/L/F-53B, significantly increased TH protein expression by 1.229-fold ($P = 0.046$) in the hippocampus (Fig. 4M, N). DAT protein expression increased by 2.940-fold ($P < 0.001$) and 1.597-fold ($P < 0.012$) in the hippocampus and cortex, at 400 μg/L of F-53B, respectively. (Fig. 4M, 4O). However, exposure to 4 and 400 μg/L had significantly increased the dopamine content (1.245-fold, $P = 0.006$; 1.313-fold, $P < 0.001$; respectively) in the hippocampus as compared with the control group (12.174 ± 2.026 ng/g) (Fig. 4P).

4. Discussion

We present the first evidence that early life exposure to F-53B alters neurobehavioral traits in children and weaning mice. In brief, F-53B was positively associated with poor WCST performance in school children, indicative of motor and learning disabilities. Furthermore, animal experiments revealed that exposure to F-53B in pregnant mice led to the transfer of F-53B through placenta and lactation to the pups, inducing neurobehavioral changes characterized by dopamine-dependent synaptogenic loss (See Fig. 5).

In this study, the median concentrations with interquartile range (IQR) of F-53B, 6:2Cl-PFESA and 8:2Cl-PFESA in children were 1.12 (0.74, 1.80), 1.10 (0.72, 1.76) and 0.02 (0.01, 0.04) ng/mL, respectively. In the present study the median concentration of 6:2Cl-PFESA in the serum of school-children, was higher than in newborns, but lower than general population (Table S7). Early-life exposure to F-53B in humans occur via the placenta (Cai et al., 2020; Chen and Yin, 2017) and breast milk (Awad et al., 2020; Jin et al., 2020a). Our study further demonstrates the presence of F-53B in the placenta and breast milk of pregnant mice, and its transmission to fetal liver and pups through placental transport and breast feeding (Table S8). Nonetheless, other potential routes of exposure include drinking water (Cui et al., 2018),

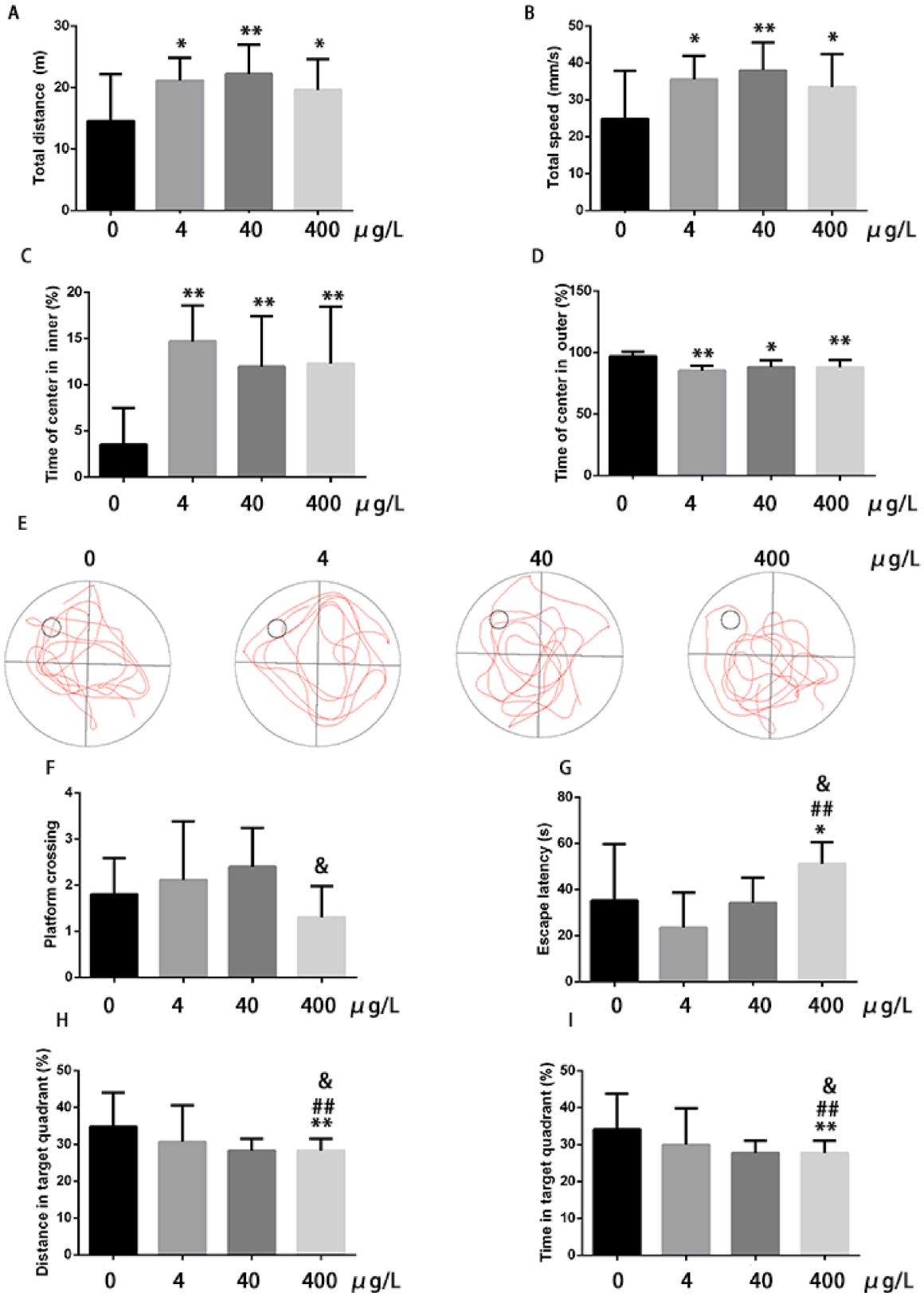

Fig. 1. Effect of F-53B exposure on motor and learning ability of weaning mice. An open field experiment was conducted to evaluate the motor ability and exploratory behavior of the weaning mice in the new environment. MWM was used to evaluate the learning ability and spatial memory ability. A-D, open filed experiment. (A) Total distance, (B) Total speed, (C) time of center in inner (%), (D) time of center in outer (%), E-I, MWM test, track of weaning mice, (F) platform crossing, (G) escape latency, (H) distance in target quadrant (%), (I) time in target quadrant (%). Data are presented as mean ± SD, (Con, M and H, n = 10; L, n = 9). $^{*}P < 0.05$, $^{**}P < 0.01$ versus control. $^{\#}P < 0.05$, $^{\#\#}P < 0.01$ versus 4 μg/L. $^{\&}P < 0.05$, $^{\&\&}P < 0.01$ versus 40 μg/L.

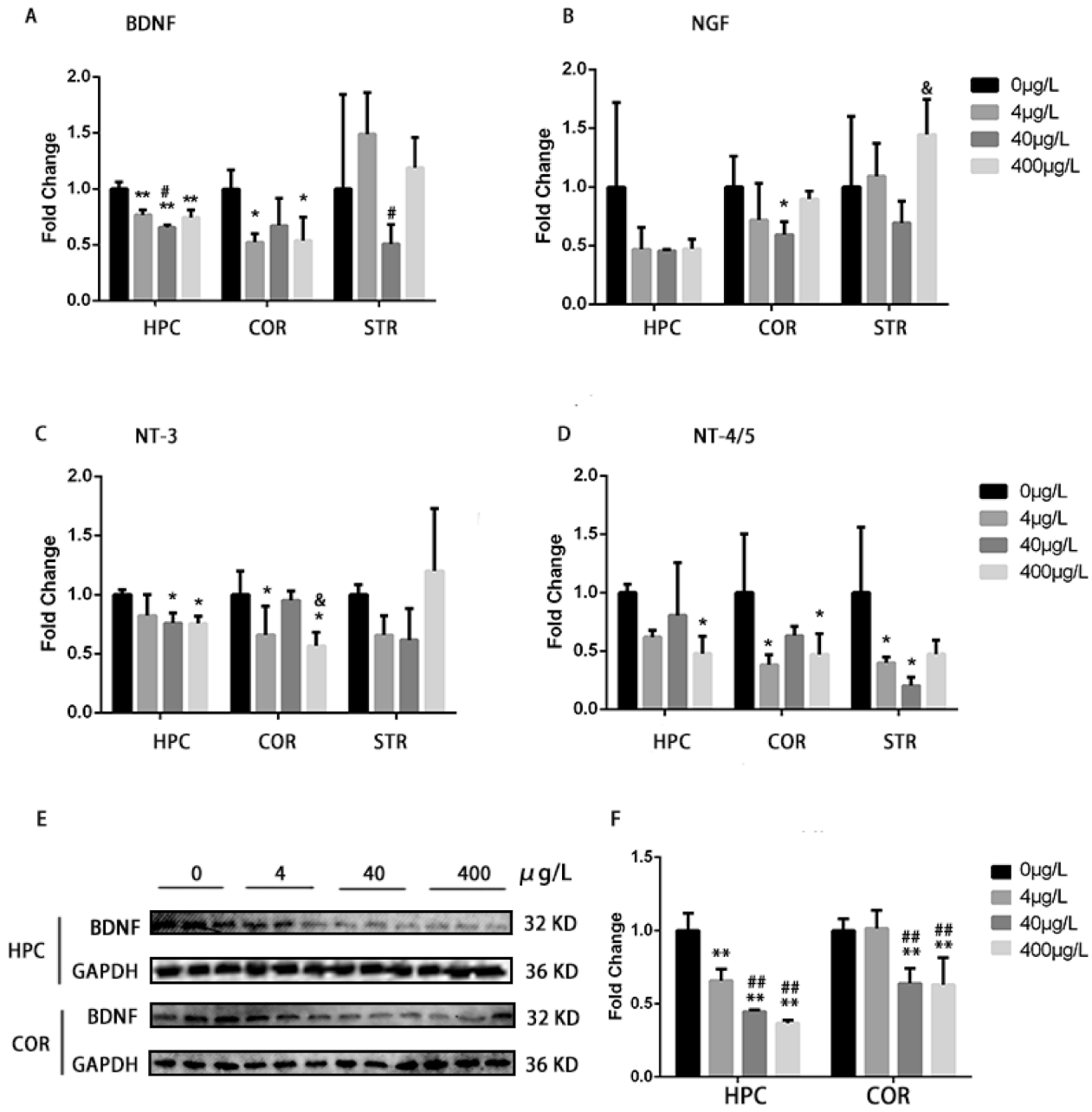

Fig. 2. Effects of F-53B exposure on neuronal development of weaning mice in different encephalic regions. A-D, the mRNA expression of BDNF, NGF, NT-3, NT-4/5 was decreased in F-53B exposure group compared with control group, detected by qRT-PCR. E, F, the protein expression of BDNF was decreased in F-53B exposure group compared with control group, detected by western blot and quantified by Image J (F). Data are presented as mean ± SD (n = 3). $^{*}P < 0.05$, $^{**}P < 0.01$ versus control. $^{\#}P < 0.05$, $^{\#\#}P < 0.01$ versus 4 μg/L. $^{\&}P < 0.05$, $^{\&\&}P < 0.01$ versus 40 μg/L.

food (Jin et al., 2020b; Zhou et al., 2020), indoor air and dust (Wang et al., 2018b; Xu et al., 2021). Notably, F-53B has a considerable elimination half-life of 10.1 to 56.4 years (Shi et al., 2016), suggesting that its presence in the body can accumulate over time. Given this cumulative nature, it is particularly important to focus on exposure during early life.

We observed that F-53B exposure was associated with neurobehavioral changes in both developing children and weaning mice. For developing children, F-53B was positively associated with poor WCST performance. After adjusting for confounders, significant negative associations were observed between F-53B and CC, CR, PCR, and PCLR, but positive associations were found for RE, NPE, PNPE, and PR in children, which reflected the ability of concept formation, sustained attention, learning, working memory and task switching (Grön, 1998; Smith et al., 1998; Sullivan et al., 1993). The same phenomenon, observed through morris maze and open field tests, were also seen in weaning mice. Meanwhile, compared with the control group, the expression of neurotrophic factors such as brain-derived neurotrophic factor (BDNF), nerve growth factor (NGF), neurotrophin-3 (NT-3), and neurotrophin-4/5 (NT-4/5) in hippocampus, cortex, and striatum, decreased after F-53B exposure. BDNF, NGF, NT-3 and NT-4/5 play a vital role in promoting neural cells growth, survival, and differentiation (Chang et al., 2019). Dysregulation of these neurotrophic factors can cause neurodevelopmental disorders such as attention deficit hyperactivity disorder (ADHD) and Tourette Syndrome (Galvez-Contreras et al., 2017; Klaffke et al., 2006). Furthermore, Yin et al., 2018 reported that exposure to F-53B even at the lowest dose (0.1 μmol/L) hampers early development of neuroectoderm as compared to PFOS (Yin et al., 2018).

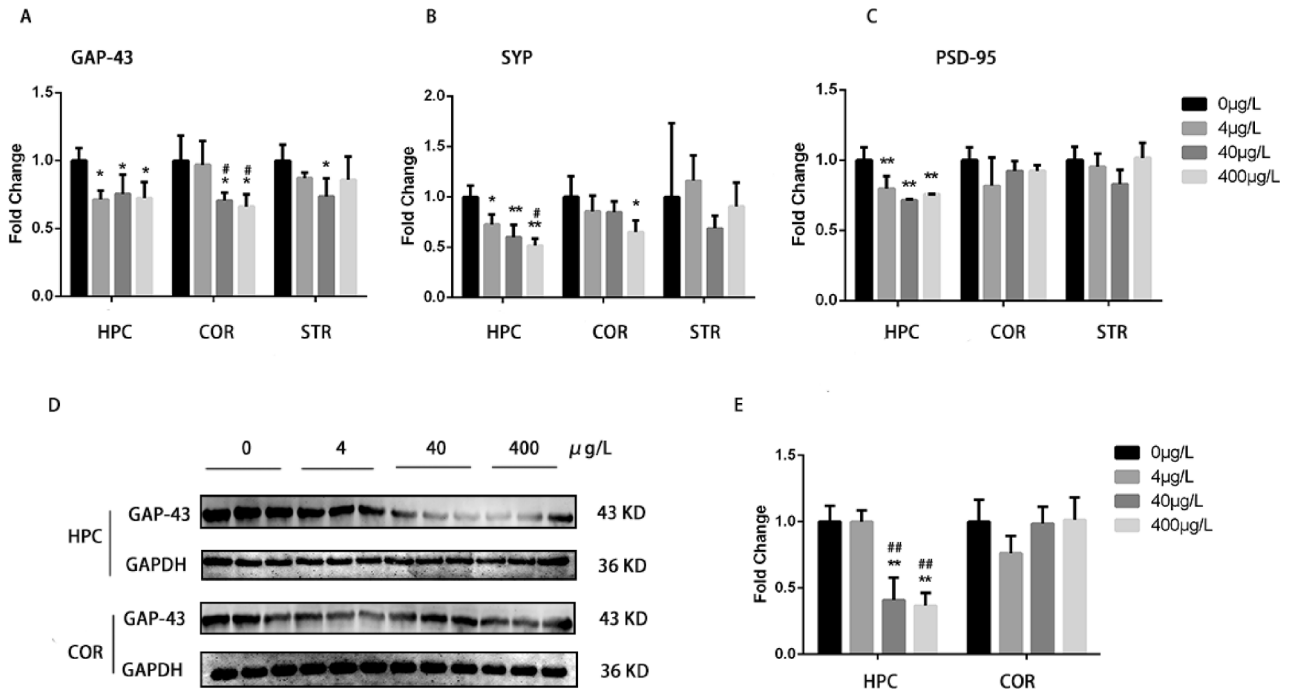

Fig. 3. Effects of F-53B exposure on synaptic plasticity of weaning mice. A-C, the mRNA expression of GAP-43, SYP, PSD-95, detected by qRT-PCR (n = 3). D, E, the protein expression of GAP-43, detected by western blot (n = 3). Data are presented as mean ± SD (n = 3). $^{*}P < 0.05$, $^{**}P < 0.01$ versus control. $^{\#}P < 0.05$, $^{\#\#}P < 0.01$ versus 4 μg/L. $^{\&}P < 0.05$, $^{\&\&}P < 0.01$ versus 40 μg/L.

In fact, exposure to F-53B and PFOS, at same exposure, significantly inhibited long-time potentiation (LTP) in rats, and F-53B irreversibly inhibited postsynaptic field excitation amplitude, which was not observed in PFOS exposure (Zhang et al., 2016). These findings show F-53B as a potential neurodevelopment toxicant and is capable of altering the learning and memory in both development children and weaning mice.

Spatial learning and memory radically rely on synaptic plasticity (Wang et al., 2015). GAP-43, SYP, and PSD-95 are involved in synaptic plasticity that plays an essential role in the regulation and renovation of the nervous system (Benowitz and Routtenberg, 1997; El-Husseini Ael et al., 2002; Li et al., 2020). In this study, the level of GAP-43, SYP, and PSD-95 decreased in weaning mice when exposed to F-53B during GD0-PND21. However, the gene expression of GAP-43 increased in the offspring larvae following by maternal exposure (without directly exposure) to 0.2, 2, 20 and 200 μg/L/F-53B, which may be contributed to compensatory (Wu et al., 2023). Nonetheless, most published literatures have reported findings similar to ours. Sprague Dawley (SD) rats when exposed to PFOS by gavage from GD0 to GD20 damaged the ultrastructure of synapses and lowered mRNA levels of synaptic vesicle associated protein in infant rats' hippocampus on PND0 and PND21 (Zeng et al., 2011a). Similarly, the SYP protein levels were also decreased in the hippocampus of offspring on PND0 and PND21, following intragastric administration of 0.1 mg/kg/bw/day of PFOS to pregnant SD mice (Zeng et al., 2011b). In another study, female SD rats exposed to a daily oral dose of 1.0 mg/kg potassium PFOS from GD0 to PND20 increased motor activity and reduced habituation in progenies on PND17 (Butenhoff et al., 2009). Likewise, female rats during pregnancy and lactation were fed with a 15 mg/L dose of PFOS by drinking water. Through prenatal and cross-fostering, pups were exposed to PFOS, which resulted in a downregulation of GAP-43 and BDNF genes on PND35 in the hippocampus (Wang et al., 2015). Thus, our findings indicate maternal exposure to F-53B disrupts synaptic plasticity in pups, as observed from the downregulation of markers genes.

Our data indicates that F-53B -induced synaptic dysregulation may be dependent on dopaminergic signaling. DA is a neurotransmitter that has vital effects on movement, learning, and memory abilities (Iversen and Iversen, 2007). DA is synthesized from tyrosine, an amino acid that is converted to L-3,4-dihydroxyphenylalanine (L-DOPA) by tyrosine hydroxylase (TH). L-DOPA is further metabolized to DA by DOPA decarboxylase (DDC). Monoamine oxidase (MAO) disintegrates dopamine into 3,4-dihydroxyphenylacetic acid (DOPAC) and then through catechol-O-methyltransferase (COMT) it is broken down into high vanillic acid (HVA) (Klein and Battagello, 2019). Once released, DA binds to the D1(DRD1, DRD5) and D2 (DRD2, DRD3, DRD4) receptors (Baik, 2013). In this study, exposure to F-53B disturbs DA metabolism, perturbation of this tightly regulated process has been linked to neurological impairments (Meng et al., 2021). Furthermore, the reduction of gene expression of DA receptors counteracts the effects of high DA levels and maintain homeostasis (Grønnestad et al., 2021). In addition, we observed downregulation of DA receptors while dopamine levels were higher in hippocampus and insignificant changes were observed in the cortex and striatum. Three published studies have measured DA level after F-53B exposure. Zebrafish embryos (2 h post-fertilization, 2-hpf) were exposed to 0.15, 1.5, and 15 μg/L of F-53B for 120-hpf, the level of dopamine increased but was statistically insignificant (Wu et al., 2022). In another study exposure to 1 μM F-53B for 21 days did not led to any observable change in DA levels of adult zebrafish (Wang et al., 2023). However, the DA content of offspring larvae (cultured without F-53B for 120-hpf) decreased following adult zebrafish exposure to 200 μg/L/F-53B (Wu et al., 2023). Given that F-53B is an alternative to PFASs, it is also easy to compare. However, the changing trend of DA after PFAS exposure is also still inconclusive. For example, northern leopard frogs exposed to PFOS and PFOA during the development period increased DA levels (Foguth et al., 2019), while opposite effects were seen in PFOS-exposed adult rats (Salgado et al., 2015) and Northern European snow PFAS mixture-exposed wild Bank voles (Grønnestad et al., 2021). Thus, the inconsistent pattern of DA levels can be attributed to various factors, including exposure window, exposure duration, PFAS type and species (Grønnestad et al., 2021). More population and animal experiments should be investigated in the future.

In this study, we studies neurotoxicity of F-53B in different brain

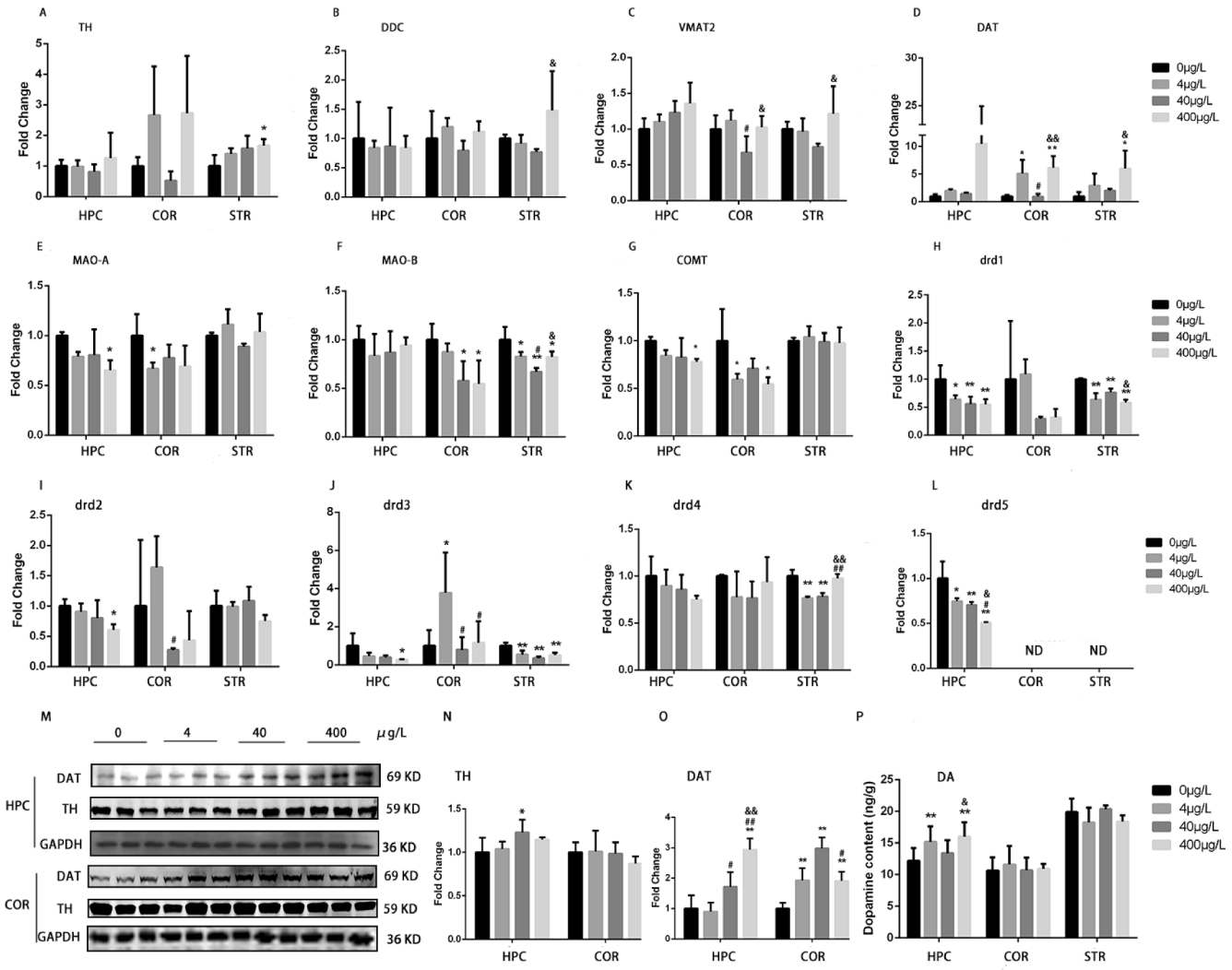

Fig. 4. Effects of F-53B exposure on DA signaling pathway of weaning mice. A-L, the mRNA expression of TH, DDC, VMAT2, DAT, MAO-A, MAO-B, COMT, DA receptor (drd1, drd2, drd3, drd4, drd5), detected by qRT-PCR (n = 3). ND: Not Detected. M–O, the protein expression of TH and DAT, detected by western blot (M) and quantified by Image J (N, O) (n = 3). (P) the DA content, detected by ELISA (for hippocampus and cortex: Con, M and H, n = 10; L, n = 9; for striatum: n = 5). Data are presented as mean ± SD (n = 3). $^{*}P < 0.05$, $^{**}P < 0.01$ versus control. $^{\#}P < 0.05$, $^{\#\#}P < 0.01$ versus 4 μg/L. $^{\&}P < 0.05$, $^{\&\&}P < 0.01$ versus 40 μg/L.

regions (i.e., hippocampus, cortex, and striatum), and our results showed that the hippocampus is the most vulnerable to F-53B exposure based on the changes of DA levels. High concentration of F-53B in the hippocampus may be the reason for that, a finding similar to a PFOS study. A previous study showed that the concentration of PFOS in hippocampus was higher than in cortex of offspring on PND0 and PND21, followed by the pregnant SD mice were intragastric with 0.1, 0.6 or 2.0 mg/kg/bw/day PFOS (Zeng et al., 2011b). On the other hand, the difference in results may also reflect event specificity. The hippocampus system is thought to be declarative or relational memory that quickly associates with novel events, whereas procedural learning, such as motor skill, sequence learning, and habit, is deemed to be regulated by cortical-striatal-cerebellar based circuit (Döhring et al., 2017).We also set three dose groups to explore the dose–response relationship. Unfortunately, our study didn't find concentration dependent effects for most indicators, which may be attributed to bioconcentration factors (BCF). Recent studies have shown that an inverted U-shaped pattern between exposure concentration of F-53B and BCF in zebrafish larvae (Tu et al., 2019). The accumulation level of F-53B might be a combination of exposure concentration and BCF. Our result data related to the concentration of placenta also show no difference between 4 μg/L and 40 μg/L (Fig.S8). However, the absorption, distribution, metabolism, and excretion of F-53B in vulnerable population such as pregnant women and babies are still unclear, more evidence should be provided in the future (Yi et al., 2022).

5. Conclusion

Exposure to F-53B is associated with poor WCST performance in children, indicative of cognitive impairment. Weaning mice exposed to F-53B show hyperactivity, reduced learning, and disrupted cognitive abilities. These effects align with disturbances in dopaminergic pathways and plasticity, accompanied by decreased neurotrophic factors in key brain regions. This suggests that exposure to F-53B is associated with adverse neurobehavior during early life, potentially mediated by dopamine-dependent synaptic changes.

CRediT authorship contribution statement

Li-Xia Liang: Software, Formal analysis, Writing – original draft, Writing – review & editing. **Jingjing Liang:** Methodology, Software, Conceptualization. **Qing-Qing Li:** Software, Conceptualization, Data curation. **Mohammed Zeeshan:** Conceptualization, Data curation, Writing – review & editing. **Zheqing Zhang:** Conceptualization, Data

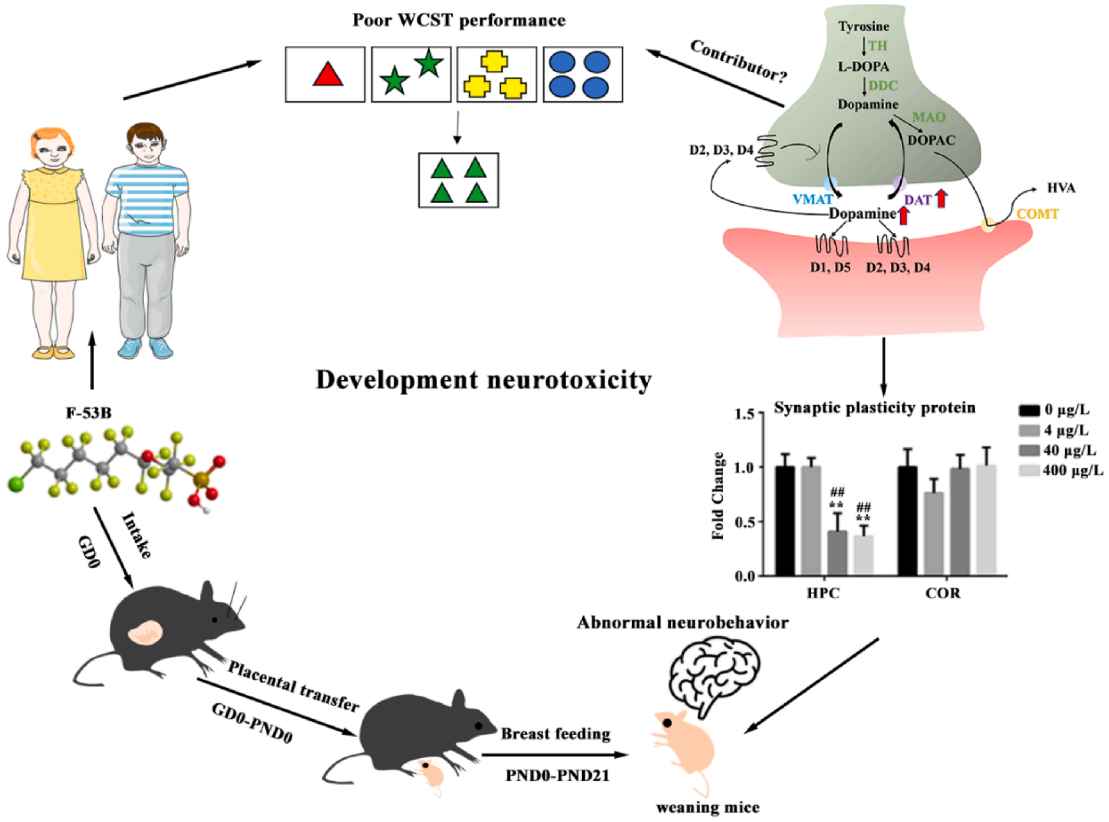

Fig. 5. Abstract figure. Exposure to F-53B is associated with early-life neurobehavioral changes, potentially via dopamine-dependent synaptic changes.

curation. **Nanxiang Jin:** Writing – review & editing. **Li-Zi Lin:** Conceptualization, Data curation, Methodology. **Lu-Yin Wu:** Data curation, Methodology. **Ming-Kun Sun:** Data curation, Software. **Wei-Hong Tan:** Methodology, Data curation. **Yang Zhou:** Data curation, Funding acquisition. **Chu Chu:** Funding acquisition. **Li-Wen Hu:** Funding acquisition. **Ru-Qing Liu:** Funding acquisition. **Xiao-Wen Zeng:** Project administration, Funding acquisition. **Yunjiang Yu:** Conceptualization, Data curation, Validation, Writing – review & editing. **Guang-Hui Dong:** Project administration, Funding acquisition, Supervision.

Declaration of Competing Interest

The authors declare that they have no known competing financial interests or personal relationships that could have appeared to influence the work reported in this paper.

Data availability

Data will be made available on request.

Acknowledgments

This work was supported by the National Natural Science Foundation of China (No.82173471; No.82003409; No. 82103823; No.82073503), the Guangxi Natural Science Foundation (2018GXNSFBA138047), the Guangxi Key Research and Development Plan (GUIKEAB18050024), Natural Science Foundation of Guangdong Province (No. 2021A1515012212; No. 2021A1515011754; No. 2021B1515020015; No. 2019A050510017).

Appendix A. Supplementary material

Supplementary data to this article can be found online at https://doi.org/10.1016/j.envint.2023.108272.

References

Ainsworth, B.E., Haskell, W.L., Herrmann, S.D., Meckes, N., Bassett Jr., D.R., Tudor-Locke, C., Greer, J.L., Vezina, J., Whitt-Glover, M.C., Leon, A.S., 2011. 2011 Compendium of Physical Activities: a second update of codes and MET values. Med. Sci. Sports Exerc. 43, 1575–1581.

Awad, R., Zhou, Y., Nyberg, E., Namazkar, S., Yongning, W., Xiao, Q., Sun, Y., Zhu, Z., Bergman, Å., Benskin, J.P., 2020. Emerging per- and polyfluoroalkyl substances (PFAS) in human milk from Sweden and China. Environ. Sci. Processes Impacts 22, 2023–2030.

Babcock, T., Dirks, B., Adeyi, B., Scheckner, B., 2012. Efficacy of lisdexamfetamine dimesylate in adults with attention-deficit/hyperactivity disorder previously treated with amphetamines: analyses from a randomized, double-blind, multicenter, placebo-controlled titration study. BMC Pharmacol. Toxicol. 13, 18.

Baik, J.H., 2013. Dopamine signaling in reward-related behaviors. Front. Neural Circuits 7, 152.

Benowitz, L.I., Routtenberg, A., 1997. GAP-43: an intrinsic determinant of neuronal development and plasticity. Trends Neurosci. 20, 84–91.

Benskin, J.P., Ikonomou, M.G., Woudneh, M.B., Cosgrove, J.R., 2012. Rapid characterization of perfluoralkyl carboxylate, sulfonate, and sulfonamide isomers by high-performance liquid chromatography-tandem mass spectrometry. J. Chromatogr. A 1247, 165–170.

Butenhoff, J.L., Ehresman, D.J., Chang, S.C., Parker, G.A., Stump, D.G., 2009. Gestational and lactational exposure to potassium perfluorooctanesulfonate (K+PFOS) in rats: developmental neurotoxicity. Reproductive toxicology (Elmsford, NY). 27, 319–330.

Cai, D., Li, Q.Q., Chu, C., Wang, S.Z., Tang, Y.T., Appleton, A.A., Qiu, R.L., Yang, B.Y., Hu, L.W., Dong, G.H., Zeng, X.W., 2020. High trans-placental transfer of perfluoroalkyl substances alternatives in the matched maternal-cord blood serum: Evidence from a birth cohort study. Sci. Total Environ. 705, 135885.

Calabresi, P., Picconi, B., Tozzi, A., Di Filippo, M., 2007. Dopamine-mediated regulation of corticostriatal synaptic plasticity. Trends Neurosci. 30, 211–219.

Chang, H.M., Wu, H.C., Sun, Z.G., Lian, F., Leung, P.C.K., 2019. Neurotrophins and glial cell line-derived neurotrophic factor in the ovary: physiological and pathophysiological implications. Hum. Reprod. Update 25, 224–242.

Chen, F., Yin, S. Chlorinated Polyfluoroalkyl Ether Sulfonic Acids in Matched Maternal, Cord, and Placenta Samples: A Study of Transplacental Transfer. 51:6387-6394; 2017.

Chen, S.S., Liao, X.M., Wei, Q.Z., Zhou, Y.Y., Su, M.Y., Hu, Y., Song, Y.Y., Zhang, Z.Q., Liang, J.J., 2022. Associations of the Gut Microbiota Composition and Fecal Short-Chain Fatty Acids with Leukocyte Telomere Length in Children Aged 6 to 9 Years in Guangzhou, China: A Cross-sectional Study. J. Nutr. 152, 1549–1559.

Cui, Q., Pan, Y., Zhang, H., Sheng, N., Dai, J. Elevated concentrations of perfluorohexanesulfonate and other per- and polyfluoroalkyl substances in Baiyangdian Lake (China): Source characterization and exposure assessment. Environ. Pollution (Barking, Essex : 1987). 241:684-691; 2018.

Dai, M., Lin, L., Liang, J., Wang, Z., Jing, J., 2019. Gender Difference in the Association Between Executive Function and Autistic Traits in Typically Developing Children. J. Autism Dev. Disord. 49, 1182–1192.

Döhring, J., Stoldt, A., Witt, K., Schönfeld, R., Deuschl, G., Born, J., Bartsch, T., 2017. Motor skill learning and offline-changes in TGA patients with acute hippocampal CA1 lesions. Cortex; J. Devoted Study Nervous Syst. Behavior. 89, 156–168.

Egan, M.F., Goldberg, T.E., Gscheidle, T., Weirich, M., Rawlings, R., Hyde, T.M., Bigelow, L., Weinberger, D.R., 2001. Relative risk for cognitive impairments in siblings of patients with schizophrenia. Biol. Psychiatry 50, 98–107.

El-Husseini Ael, D., Schnell, E., Dakoji, S., Sweeney, N., Zhou, Q., Prange, O., Gauthier-Campbell, C., Aguilera-Moreno, A., Nicoll, R.A., Bredt, D.S., 2002. Synaptic strength regulated by palmitate cycling on PSD-95. Cell 108, 849–863.

Foguth, R.M., Flynn, R.W., de Perre, C., Iacchetta, M., Lee, L.S., Sepúlveda, M.S., Cannon, J.R., 2019. Developmental exposure to perfluorooctane sulfonate (PFOS) and perfluorooctanoic acid (PFOA) selectively decreases brain dopamine levels in Northern leopard frogs. Toxicol. Appl. Pharmacol. 377, 114623.

Galvez-Contreras, A.Y., Campos-Ordonez, T., Gonzalez-Castaneda, R.E., Gonzalez-Perez, O., 2017. Alterations of Growth Factors in Autism and Attention-Deficit/Hyperactivity Disorder. Front. Psych. 8, 126.

Grön, G., 1998. Auditory and visual working memory performance in patients with frontal lobe damage and in schizophrenic patients with low scores on the Wisconsin Card Sorting Test. Psychiatry Res. 80, 83–96.

Grønnestad, R., Schlenk, D., Krøkje, Å., Jaspers, V.L.B., Jenssen, B.M., Coffin, S., Bertotto, L.B., Giroux, M., Lyche, J.L., Arukwe, A., 2021. Alteration of neuro-dopamine and steroid hormone homeostasis in wild Bank voles in relation to tissue concentrations of PFAS at a Nordic skiing area. Sci. Total Environ. 756, 143745.

Hallgren, S., Viberg, H., 2016. Postnatal exposure to PFOS, but not PBDE 99, disturb dopaminergic gene transcription in the mouse CNS. Environ. Toxicol. Pharmacol. 41, 121–126.

He, Y., Lv, D., Li, C., Liu, X., Liu, W., Han, W., 2022. Human exposure to F-53B in China and the evaluation of its potential toxicity: An overview. Environ. Int. 161, 107108.

Health Effects Support Document for Perfluorooctane Sulfonate (PFOS). Ofce of Water EPA 822-R-16-002 May 2016, 245p.

Huang, Y.Y.; Simpson, E.; Kellendonk, C.; Kandel, E.R. Genetic evidence for the bidirectional modulation of synaptic plasticity in the prefrontal cortex by D1 receptors. Proceedings of the National Academy of Sciences of the United States of America. 101:3236-3241; 2004.

Iversen, S.D., Iversen, L.L., 2007. Dopamine: 50 years in perspective. Trends Neurosci. 30, 188–193.

Jin, Q., Ma, J., Shi, Y., Chen, C., Wang, Y., Zhao, E., Cai, Y., Qu, G., 2020a. Biomonitoring of chlorinated polyfluoroalkyl ether sulfonic acid in the general population in central and eastern China: Occurrence and associations with age/sex. Environ. Int. 144, 106043.

Jin, Q., Shi, Y., Cai, Y., 2020b. Occurrence and risk of chlorinated polyfluoroalkyl ether sulfonic acids (Cl-PFESAs) in seafood from markets in Beijing, China. Sci. Total Environ. 726, 138538.

Klaffke, S., König, I.R., Poustka, F., Ziegler, A., Hebebrand, J., Bandmann, O., 2006. Brain-derived neurotrophic factor: a genetic risk factor for obsessive-compulsive disorder and Tourette syndrome? Movement Disorders: Off. J. Move. Dis. Soc. 21, 881–883.

Klein, M.O., Battagello, D.S., 2019. Dopamine: Functions. Signal., Assoc. Neurol. Dis. 39, 31–59.

Lai, K.P., Lee, J.C., 2017. Effects of in Utero PFOS Exposure on Transcriptome. Lipidome, and Function of Mouse Testis. 51, 8782–8794.

Li, S., Cullen, W.K., Anwyl, R., Rowan, M.J., 2003. Dopamine-dependent facilitation of LTP induction in hippocampal CA1 by exposure to spatial novelty. Nat. Neurosci. 6, 526–531.

Li, J., Liu, M., Gao, J., Jiang, Y., Wu, L., Cheong, Y.K., Ren, G., Yang, Z., 2020. AVNP2 protects against cognitive impairments induced by C6 glioma by suppressing tumour associated inflammation in rats. Brain Behav. Immun. 87, 645–659.

Liu, J.; Gao, X.; Wang, Y.; Leng, J.; Li, J.; Zhao, Y.; Wu, Y., 2021. Profiling of emerging and legacy per-/polyfluoroalkyl substances in serum among pregnant women in China. Environmental pollution (Barking, Essex : 1987). 271:116376; 2021.

Liu, H.-X., Huang, Y., Pan, Y.-T., Sun, X.-J., Li, Y.-Y., Zhou, A.-F., Dai, J.-Y., Li, H., Xu, S.-Q., Lu, S., 2022. Associations between emerging chlorinated polyfluoroalkyl ether sulfonic acids exposure and birth size. Hygiene and Environmental Health Advances 4, 100034.

Liu, W., Qin, H., Li, J., Zhang, Q., Zhang, H., Wang, Z., He, X., 2017. Atmospheric chlorinated polyfluorinated ether sulfonate and ionic perfluoroalkyl acids in 2006 to 2014 in Dalian, China. Environ. Toxicol. Chem. 36, 2581–2586.

Lu, Y., Meng, L., Ma, D., Cao, H., Liang, Y., Liu, H., Wang, Y., Jiang, G., 2021. The occurrence of PFAS in human placenta and their binding abilities to human serum albumin and organic anion transporter 4. Environmental pollution (Barking, Essex : 1987). 273:116460.

MacInnis, J.J., Lehnherr, I., Muir, D.C.G., Quinlan, R., De Silva, A.O., 2019. Characterization of perfluoroalkyl substances in sediment cores from High and Low Arctic lakes in Canada. Sci. Total Environ. 666, 414–422.

Meng, H.R., Suenaga, T., Edamura, M., Fukuda, A., Ishida, Y., Nakahara, D., Murakami, G., 2021. Functional MHCI deficiency induces ADHD-like symptoms with increased dopamine D1 receptor expression. Brain Behav. Immun. 97, 22–31.

Ruan, T., Lin, Y., Wang, T., Liu, R., Jiang, G., 2015. Identification of Novel Polyfluorinated Ether Sulfonates as PFOS Alternatives in Municipal Sewage Sludge in China. Environ. Sci. Tech. 49, 6519–6527.

Rubia, K., Halari, R., Mohammad, A.M., Taylor, E., Brammer, M., 2011. Methylphenidate normalizes frontocingulate underactivation during error processing in attention-deficit/hyperactivity disorder. Biol. Psychiatry 70, 255–262.

Salgado, R., Pereiro, N., López-Doval, S., Lafuente, A., 2015. Initial study on the possible mechanisms involved in the effects of high doses of perfluorooctane sulfonate (PFOS) on prolactin secretion. Food Chem. Toxicol. 83, 10–16.

Sheng, N., Wang, J., Guo, Y., Wang, J., 2020. Interactions of Perfluorooctanesulfonate and 6:2 Chlorinated Polyfluorinated Ether Sulfonate with Human Serum Albumin. A Comparative Study. 33, 1478–1486.

Shi, Y., Vestergren, R., Xu, L., Zhou, Z., Li, C., Liang, Y., Cai, Y., 2016. Human Exposure and Elimination Kinetics of Chlorinated Polyfluoroalkyl Ether Sulfonic Acids (Cl-PFESAs). Environ. Sci. Tech. 50, 2396–2404.

Smith, G.L., Large, M.M., Kavanagh, D.J., Karayanidis, F., Barrett, N.A., Michie, P.T., O'Sullivan, B.T., 1998. Further evidence for a deficit in switching attention in schizophrenia. J. Abnorm. Psychol. 107, 390–398.

Sullivan, E.V., Mathalon, D.H., Zipursky, R.B., Kersteen-Tucker, Z., Knight, R.T., Pfefferbaum, A., 1993. Factors of the Wisconsin Card Sorting Test as measures of frontal-lobe function in schizophrenia and in chronic alcoholism. Psychiatry Res. 46, 175–199.

Tu, W.; Martínez, R.; Navarro-Martin, L.; Kostyniuk, D.J.; Hum, C.; Huang, J.; Deng, M.; Jin, Y. Bioconcentration and Metabolic Effects of Emerging PFOS Alternatives in Developing Zebrafish. 53:13427-13439; 2019.

Umegaki, H., Munoz, J., Meyer, R.C., Spangler, E.L., Yoshimura, J., Ikari, H., Iguchi, A., Ingram, D.K., 2001. Involvement of dopamine D(2) receptors in complex maze learning and acetylcholine release in ventral hippocampus of rats. Neuroscience 103, 27–33.

Wang, J., Pan, Y., Cui, Q., Yao, B., Wang, J. Penetration of PFASs Across the Blood Cerebrospinal Fluid Barrier and Its Determinants in Humans. 52:13553-13561; 2018a.

Wang, Q., Gu, X., Liu, Y., Liu, S., Lu, W., Wu, Y., Lu, H., Huang, J., Tu, W., 2023. Insights into the circadian rhythm alterations of the novel PFOS substitutes F-53B and OBS on adult zebrafish. J. Hazard. Mater. 448, 130959.

Wang, S., Huang, J., Yang, Y., Hui, Y., Ge, Y., Larssen, T., Yu, G., Deng, S., Wang, B., Harman, C., 2013. First report of a Chinese PFOS alternative overlooked for 30 years: its toxicity, persistence, and presence in the environment. Environ. Sci. Tech. 47, 10163–10170.

Wang, Y., Liu, W., Zhang, Q., Zhao, H., Quan, X., 2015. Effects of developmental perfluorooctane sulfonate exposure on spatial learning and memory ability of rats and mechanism associated with synaptic plasticity. Food Chem. Toxicol. 76, 70–76.

Wang, Y., Shi, Y., Vestergren, R., Zhou, Z., Liang, Y., Cai, Y., 2018b. Using hair, nail and urine samples for human exposure assessment of legacy and emerging per- and polyfluoroalkyl substances. Sci. Total Environ. 636, 383–391.

Wu, L., Zeeshan, M., Dang, Y., Liang, L.Y., Gong, Y.C., Li, Q.Q., Tan, Y.W., Fan, Y.Y., Lin, L.Z., Zhou, Y., Liu, R.Q., Hu, L.W., Yang, B.Y., Zeng, X.W., Yu, Y., Dong, G.H., 2022. Environmentally relevant concentrations of F-53B induce eye development disorders-mediated locomotor behavior in zebrafish larvae. Chemosphere 308, 136130.

Wu, L., Zeeshan, M., Dang, Y., Zhang, Y.T., Liang, L.X., Huang, J.W., Zhou, J.X., Guo, L. H., Fan, Y.Y., Sun, M.K., Yu, T., Wen, Y., Lin, L.Z., Liu, R.Q., Dong, G.H., Chu, C., 2023. Maternal transfer of F-53B inhibited neurobehavior in zebrafish offspring larvae and potential mechanisms: Dopaminergic dysfunction, eye development defects and disrupted calcium homeostasis. Sci. Total Environ. 894, 164838.

Xu, F., Chen, D., Liu, X., Guan, Q., Tan, H., Zhou, D., Shi, Y., Liu, J., Hu, Y., 2021. Emerging and legacy per- and polyfluoroalkyl substances in house dust from South China: Contamination status and human exposure assessment. Environ. Res. 192, 110243.

Yi, S., Yang, D., Zhu, L. Significant Reductive Transformation of 6:2 Chlorinated Polyfluorooctane Ether Sulfonate to Form Hydrogen-Substituted Polyfluorooctane Ether Sulfonate and Their Toxicokinetics in Male Sprague-Dawley Rats. 56:6123-6132; 2022.

Yin, N., Yang, R., Liang, S., Liang, S., Hu, B., Ruan, T., Faiola, F., 2018. Evaluation of the early developmental neural toxicity of F-53B, as compared to PFOS, with an in vitro mouse stem cell differentiation model. Chemosphere 204, 109–118.

Yuan, S., Tong, W., Zheng, T., Zhu, X., Tang, B., Dang, Y., Letcher, R.J., Liu, C., 2022. Establishment of a behavioral model to study effects of typical chemicals toward zebrafish larvae. Hygiene and Environmental Health Advances 4, 100021.

Zeng, H.C., Li, Y.Y., Zhang, L., Wang, Y.J., Chen, J., Xia, W., Lin, Y., Wei, J., Lv, Z.Q., Li, M., Xu, S.Q., 2011a. Prenatal exposure to perfluorooctanesulfonate in rat resulted in long-lasting changes of expression of synapsins and synaptophysin. Synapse (New York, NY). 65, 225–233.

Zeng, H.C., Zhang, L., Li, Y.Y., Wang, Y.J., Xia, W., Lin, Y., Wei, J., Xu, S.Q., 2011b. Inflammation-like glial response in rat brain induced by prenatal PFOS exposure. Neurotoxicology 32, 130–139.

Zhang, Q., Liu, W., Niu, Q., Wang, Y., Zhao, H., Zhang, H., Song, J., Tsuda, S., Saito, N., 2016. Effects of perfluorooctane sulfonate and its alternatives on long-term potentiation in the hippocampus CA1 region of adult rats in vivo. Toxicol. Res. 5, 539–546.

Zhou, C.C., Gao, Z.Y., He, Y.Q., Wu, M.Q., Chen, F., Wang, J., Liu, J.X., Yan, C.H., 2019a. Effects of lead, mercury, aluminium and manganese co-exposure on the serum BDNF

concentration of pre-school children in Taizhou. China. Chemosphere. 217, 158–165.
Zhou, J., Li, Z., Guo, X., Li, Y., Wu, Z., Zhu, L., 2019b. Evidences for replacing legacy per- and polyfluoroalkyl substances with emerging ones in Fen and Wei River basins in central and western China. J. Hazard. Mater. 377, 78–87.
Zhou, J., Li, M., Li, J., Shao, Z., Liu, Y., Wang, T., 2020. Bioavailability and Bioaccumulation of 6:2 Fluorotelomer Sulfonate, 6:2 Chlorinated Polyfluoroalkyl Ether Sulfonates, and Perfluorophosphinates in a Soil-Plant. System 68, 4325–4334.